

# Collection of diesel exhaust particle using electrostatic charging prior to DPF and regeneration of DPF using sliding discharge

Hideaki Hayashi  
Dept. Environmental and  
Life Sciences  
Toyohashi University of  
Technology  
Japan  
h063822@edu.imc.tut.ac.jp

Kazunori Takashima  
Dept. Environmental and  
Life Sciences  
Toyohashi University of  
Technology  
Japan  
takashima@ens.tut.ac.jp

Akira Mizuno  
Dept. Environmental and  
Life Sciences  
Toyohashi University of  
Technology  
Japan  
mizuno@ens.tut.ac.jp

## Abstract:

Diesel particulate filter (DPF) has been established as a key technology in reducing diesel particulate emission. However, technological improvements to pressure drop, durability, and insufficient collection efficiency for nano-particles are still required. Electrostatic precipitator (ESP) is another leading technology used in exhaust treatment but it is currently limited to applications for stationary sources. In this paper we have proven that simultaneous use of ESP and DPF show synergetic effects of very high collection efficiency and slower increase of the pressure drop. The number concentration of particles observed downstream of the combined system was 98% smaller compared with that of DPF only. At the same time, it was confirmed that increase in the pressure drop across the DPF was slower about 10% compared with that of DPF only. In addition, regeneration of DPF was also investigated using non-thermal plasma (NTP). In order to generate the plasma inside the DPF, a surface discharge was used in front and a DC electric field was applied across the DPF. In this study, the discharge plasma was used to oxidize PM accumulated inside the DPF. It showed around ten grams per kilowatt-hour (g/kWh) of the PM oxidation efficiency.

## 1 Introduction

The demand for more efficient automobiles has increased due to the sharp increase in oil price. In the meantime, strong economic growth in several countries has caused serious air pollution due to exhaust from vehicles. Suspended particulate matter (SPM) and nitrogen oxide ( $\text{NO}_x$ ) are main pollutants. SPM is a particle smaller than 10  $\mu\text{m}$  suspended in the atmosphere for a long time [1]. DPF has been widely used to prevent emission of SPM. Although this method has a high particulate matter (PM) collection efficiency, it still has many problems such as high pressure drop and durability during regeneration of collected soot by combustion. ESP is another technology for removing particles, and it has been used satisfactorily for cleaning of flue gas from large-capacity factories, combustion furnaces and thermal power plants. However a problem with ESP is an abnormal dust re-entrainment. Using ESP, SPM agglomerates to large particles [2]. The agglomerated particles repeat jumping and emitting from ESP. Combination of ESP and a DPF could improve collection efficiency and the increase in the pressure drop can be

slower due to agglomeration. In this paper, characteristics of an ESP-DPF combined system are reported. In addition, the situation of collected particles in a mock filter was observed by using a scanning electron microscope (SEM) to evaluate the influence of the particles charged in an ESP, due to the difficulty in observing particles collected on the surface of DPF.

On the other hand, in order to develop a self-consistent aftertreatment system, it is also very important to consider DPF regeneration or the removal of PM deposit. Oxidation using an afterburner or a electric heater is the most typical regeneration process [3]. However, the temperature of the DPF must be 600°C or higher during these regeneration. Therefore it is possible to damage the DPF when the oxidation of the collected PM on the filter gets out of control and the temperature of the DPF becomes too high. For this reason, a novel low-temperature regeneration technology has been required.

To cope with this problem, a new method of regeneration using non-thermal plasma has been developed [4]. Since the discharge plasma can generate reactive species such as ozone, the regeneration without thermal

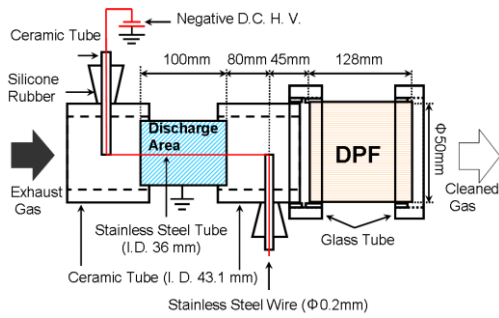


Fig. 1: ESP and DPF combined system

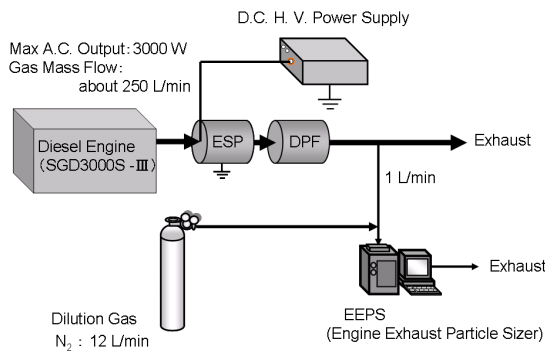


Fig. 2: Experimental Setup for the ESP and DPF combined system

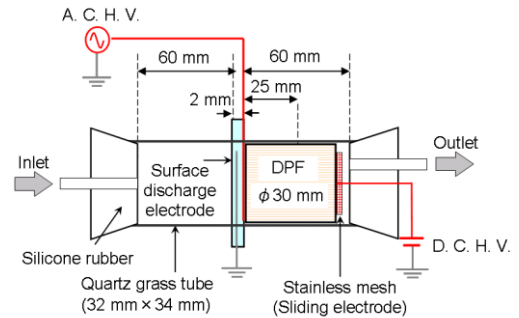
loading is expected. Recently, generation of non-thermal plasma inside honeycomb-shaped ceramic using sliding discharge has been made possible [5,6]. The sliding discharge is a discharge generated on a dielectric surface by a combination of AC and DC powers in three-electrode geometry [7]. The discharge is a product of AC-driven barrier discharge “sliding” along the dielectrics when the DC component is applied to the remote third electrode. Using the sliding discharge, synergic effect of plasma and catalytic reaction for  $\text{NO}_x$  reduction in selective catalytic reduction (SCR) system has been reported [8].

In order to generate the plasma inside the fine channels of the DPF, surface discharge was used in front and a DC electric field was applied across the DPF. Here, we have characterized the oxidation efficiency of this regeneration reactor.

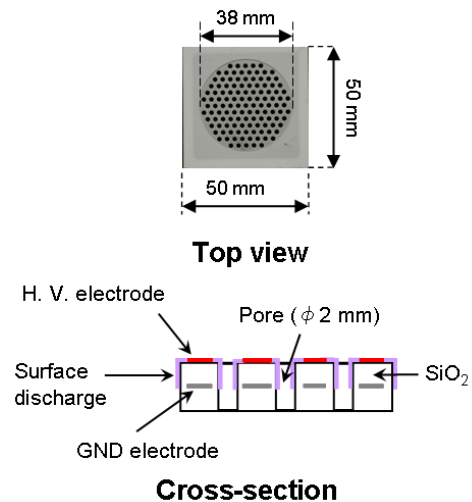
## 2 Experimental setup

### 2.1 Collection of diesel exhaust particle (DEP) using ESP and DPF combined system

Figure 1 shows the schematic illustration of the precipitator. The discharge electrode (stainless steel wire ( $\phi 0.2$  mm)) was energized with the negative D.C. high voltage. A stainless steel tube (36 mm inside diameter, 38 mm



(a) Regeneration reactor of DPF using sliding discharge



(b) Surface discharge electrode

Fig. 3: Schematic illustration of regeneration system for DPF

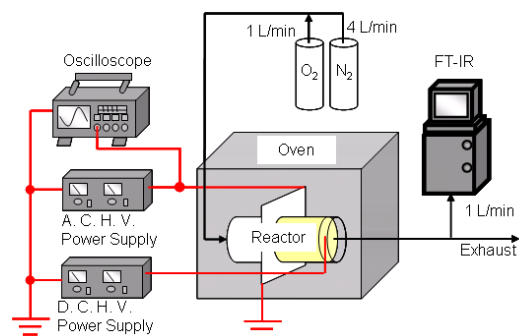


Fig. 4: Experimental setup for the regeneration system for DPF

outside diameter) was used as a collection electrode. A ceramic tube (43.1 mm inside diameter, 50 mm outside diameter) was used as an insulator. In the ESP, the length of the discharge area is 100 mm, the gas residence time was 0.024 second, and the temperature of the exhaust was  $70^\circ\text{C}$ . Because of limitation of insulating materials of the ESP used in this preliminary study to check the effect of charging, the measurements were conducted

at this temperature. The ESP was installed in front of the DPF (diameter 50 mm, length 128 mm) at about 5 m downstream from the engine.

Figure 2 shows the schematic diagram of the experimental setup for the ESP and DPF combined system. The exhaust gas from a diesel engine generator (FUJI HEAVY INDUSTRIES Ltd., SGD3000S-III) of 3 kW capacity was used with a high load of 2.6 kW in order to reduce the ratio of soluble organic fraction (SOF). SOF consists of unburned fuel and lubricant. 250 L/min of the exhaust gas was passed through the precipitator. The collection efficiency was evaluated by measuring number concentration and size distribution of the particles using an engine exhaust particle sizer (EEPS) (TSI Ltd, 3090). For the measurement, the exhaust sample was diluted by 50 times with nitrogen gas from the cylinder (12 L/min). The pressure drop across the DPF was also measured with a pressure gauge.

To prepare the samples for SEM observation, 39 L of exhaust gas from the ESP was filtered with a quartz fiber filter instead.

## 2.2 Regeneration of DPF using sliding discharge

Figure 3 shows the schematic illustration of the DPF regeneration system. Surface discharge was generated as preceding discharge. DPF was inserted into the quartz glass tube. A stainless steel mesh (16 mesh) was placed on the opposite side of the surface discharge electrode. This stainless steel mesh was connected to a DC power supply to generate the sliding discharge inside the fine channel. When DC high voltage was applied, the inside of the DPF was ionized, as if the surface discharge generated by the AC power supply were elongated by the DC electric field.

In this study, the discharge plasma was applied for the oxidation of accumulated PM inside the DPF (diameter 30 mm, length 25 mm). The condition of exhaust gas from a diesel engine was same as above. Exhaust gas from a diesel engine was supplied with 20 L/min of the flow rate to the reactor by an air pump. Diesel exhaust particles were accumulated into the DPF for 30 min before the regeneration experiment.

Figure 4 shows the experimental setup for the regeneration system of DPF. The gas flow rate was controlled by mass flow controllers. In this study, nitrogen gas flow rate was 4 L/min and oxygen gas flow rate was 1 L/min. The outlet gas from the regeneration reactor was

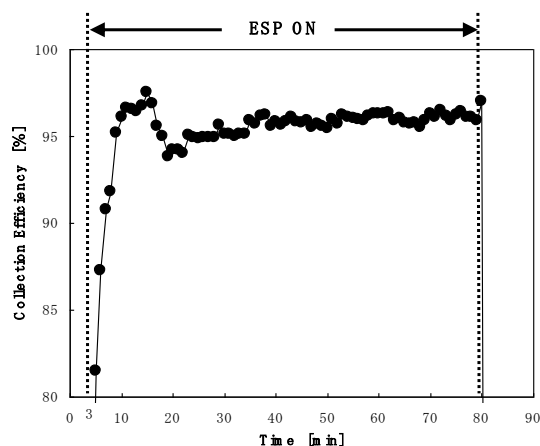


Fig. 5: The change in particles collection efficiency with ESP alone. Applied voltage: -12.5 kV

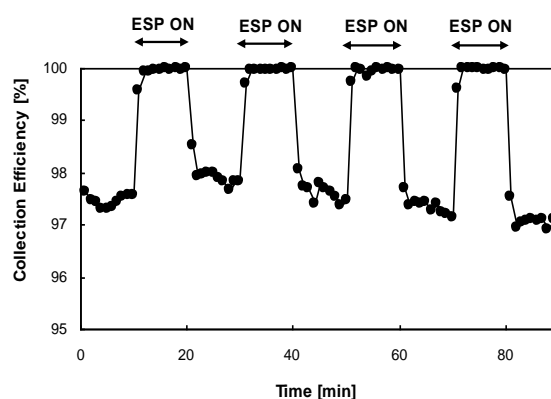


Fig. 6: Particle collection efficiency with ESP + DPF. Applied voltage: -12.5 kV

analyzed by using a fourier transform infrared spectroscope (FT-IR). The regeneration reactor was placed in a convection oven in order to control the ambient temperature.

A DC high voltage power supply (Pulse Electronic Engineering Co., Ltd. HDV-50K3SUD) and an AC high voltage power supply (TREK Model 20/20C High Voltage Amplifier) equipped with a function generator (KENWOOD OSCILLATOR AG-204D) were used. The waveform of the applied voltage was measured using a digital oscilloscope (Tektronix TDS 2014) equipped with a high voltage probe (Tektronix P6015).

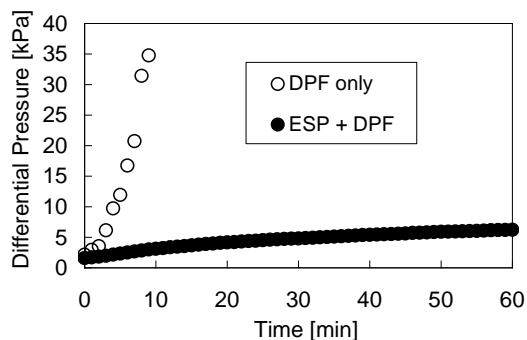


Fig. 7: Pressure drops of DPF and combined ESP/DPF. Applied voltage: -12.5 kV

### 3 Results and Discussion

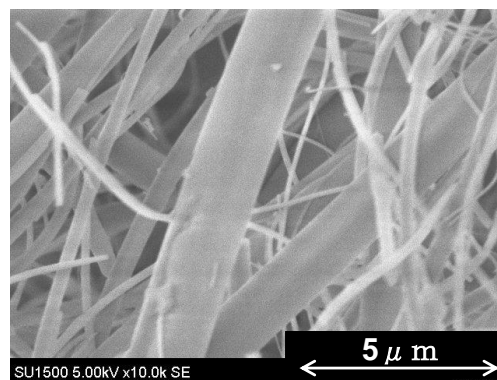
#### 3.1 Collection of diesel exhaust particle (DEP) using ESP and DPF combined system

Figure 5 shows the particle collection efficiency when only ESP was used. The size distribution measurement of the DEP without the ESP showed that the highest number concentration of particles was observed at 69.8 nm in diameter (data not shown). The collection efficiency shown here, therefore, was calculated for these particles. The ESP was operated with constant applied voltage of -12.5 kV and current was between -0.45 mA ~ -1.25 mA. ESP was turned on at 3 minutes after starting the measurement to 80 minutes. The collection efficiency was calculated by counting particles with and without the ESP operation. Figure 5 shows that the collection efficiency was about 95% or more.

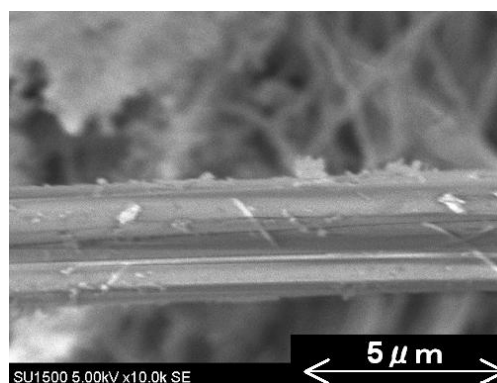
Figure 6 shows the collection efficiency when the DPF was added after the ESP and the ESP was switched on and off every 10 minutes. The applied voltage was -12.5 kV and current was -0.5 mA ~ -1.2 mA. The figure shows that the collection efficiency of the particles with and without the ESP on were nearly 100% and 98% respectively. These results suggest that the effectiveness of the simultaneous use of ESP and DPF for the particles collection.

From figures 5 and 6, it is clear that the collection efficiency is higher with the ESP on. A plausible reason is agglomeration of conductive particles in the ESP [2]. Due to abnormal re-entrainment, conductive particles are easily agglomerated in an ESP. Such large particles are easy to be trapped by a DPF. We consider that this phenomenon is an important factor leading to the high collection efficiency.

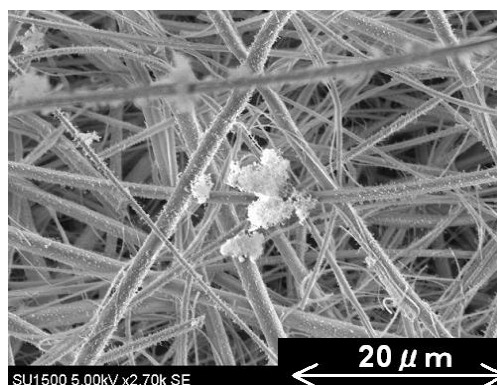
Figure 7 is the time lapse change of the



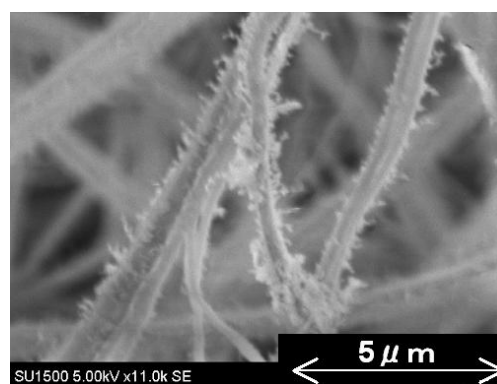
(a)



(b)



(c)



(d)

Fig. 8: Microscopic observation of collected particles on a filter set after the ESP. (a)New filter. (b)ESP off and an exposure time of 3 min. (c)ESP on and exposure time of 3 min. (d)Magnified image of (c)

pressure drop of the DPF with and without the energization of the ESP. The applied voltage; -12.5 kV, current; -0.65 mA ~ -0.87 mA. The pressure drop started to increase after the engine was on. The pressure drop increased rapidly and reached to about 35 kPa after 9 minutes without ESP. With the ESP on, the pressure drop rose significantly slower. The cause of this could be the collection of particles in the ESP, as well as the difference in the deposition behavior of the agglomerated particles on the wall of DPF.

Using SEM the state of the particles collected on the glass fiber filter set downstream of the ESP with the applied voltage of -12.5 kV (and current was -0.70 mA) was observed as shown in Figure 8.

Figure 8(a) is a new filter. Figure 8(b), is the particles collected without ESP operation. In Figure 8(b), many particles in round form were found. Figure 8(c) and (d) shows the samples with the ESP on. Figure 8(c) shows agglomerated particles on the quartz fiber filter. This figure clearly shows that particles emitted from the ESP agglomerated to be a large particle. Such large particles are easy to be trapped by the DPF. It is also expected that the agglomerated large particles are less closely accumulated on the DPF probably resulting in lower pressure drop. Therefore, this is an important factor leading to the high collection efficiency and low pressure drop. In Figure 8(d), with magnified observation, pearl-chain formation of particles was confirmed, suggesting the existence of the electric field around the filter fibers. This is a phenomenon not seen in Figure 8(b). This microscopic observation shows the effectiveness of charging particles prior to mechanical filtration.

### 3.2 Regeneration of DPF by sliding discharge

Table 1 shows the experimental condition of the regeneration of DPF. In this study, the effects of voltages applied to both surface discharge and sliding discharge electrodes, ambient temperature, and the applied frequency of the surface discharge were experimentally examined. The oxidation

Table 1: Experimental condition

| Parameters   | Value              |
|--|--------------------|
| Applied voltage at <b>surface</b> discharge electrode [kV <sub>p-p</sub> ] | 8, 10, 12          |
| Frequency [kHz]  | 0.5, 1.0, 1.5, 2.0 |
| Applied voltage at <b>sliding</b> discharge electrode [kV]                 | 4, 8               |
| Temperature [°C]   | 25, 90, 125, 150   |
| Treatment time [min]   | 30                 |

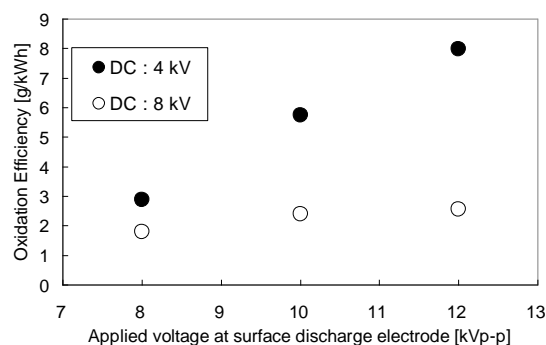


Fig. 9: Oxidation efficiency versus applied voltage at surface discharge electrode with different applied voltage at sliding discharge electrode. Frequency at surface discharge electrode: 1.0 kHz, Ambient temperature: 25 °C

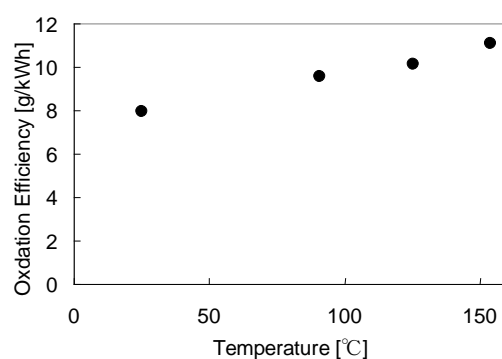


Fig. 10: Oxidation efficiency versus ambient temperature. Applied voltage: AC 12 kV<sub>p-p</sub> 1.0 kHz and DC 4 kV

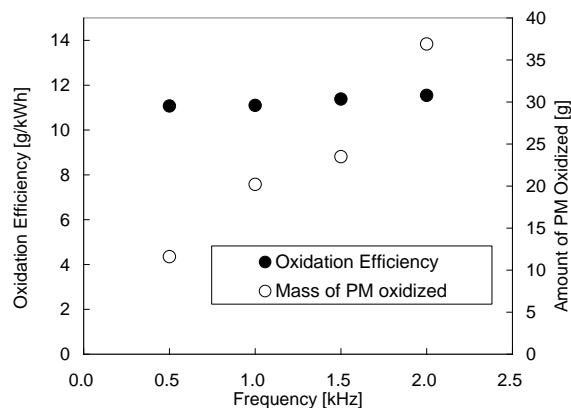


Fig. 11: Oxidation efficiency and amount of PM oxidized versus the applied frequency of the surface discharge electrode. Applied voltage: AC 12 kV<sub>p-p</sub> and DC 4 kV, Ambient temperature: 150 °C, Treatment time: 30 minutes

efficiency was calculated from the weight change of the DPF before and after the regeneration.

Figure 9 shows the correlation of oxidation efficiency and applied voltage to the surface discharge electrode for two different voltages applied to the sliding electrode: DC 4 kV and DC 8 kV. Gas flow rate was 5 L/min, ambient

temperature was 25°C, and the frequency of surface discharge was 1.0 kHz in this experiment. Not depending on the DC high voltages, the oxidation efficiency increased in proportion to the applied voltage at the surface discharge electrode. Therefore, it was confirmed that DPF was regenerated by using a sliding discharge. The oxidation efficiency was higher for DC 4 kV than that of DC 8 kV at the all experimental points of the applied voltage for surface discharge. These results suggest that the sliding discharge was affected mainly by AC voltage. In this case, the DC voltage was 4 kV.

Figure 10 shows the oxidation efficiency versus ambient temperature. Gas flow rate was 5 L/min at room temperature. The applied voltage and the frequency of the surface discharge electrode were fixed at 12 kV<sub>p-p</sub> and 1.0 kHz, respectively. The applied voltage of the sliding discharge electrode was fixed at 4 kV in this experiment. The oxidation efficiency increased with increasing the ambient temperature. Oxidation efficiency was more than 11 g/kWh at 150°C. We considered that ozone produced by surface discharge and sliding discharge was activated by increasing the ambient temperature.

Figure 11 shows the oxidation efficiency and the amount of PM oxidized versus the frequency of the voltage applied to surface discharge electrode. Gas flow rate was 5 L/min, and the ambient temperature was 154°C, the applied voltage and frequency of the surface discharge electrode were fixed at 12 kV<sub>p-p</sub> respectively. The DC applied voltage of the sliding discharge electrode was fixed at 4 kV in this experiment. This result shows that frequency of the AC high voltage does not effect the efficiency. However, the amount of PM oxidized in a fixed discharge time increased in proportion to frequency suggesting that the intensity of the sliding discharge increased with the frequency of AC voltage.

## 4 Conclusion

The combination of the ESP and the DPF showed effective collection of nanoparticles. The pressure drop of the DPF increased slowly with the combined system. The electron microscopic observation of the particles sampled downstream of an ESP showed a pearl-chain formation of the particles. This change in a macroscopic form of the particles could be a reason for the slow rise of the pressure drop. DPF was regenerated by using

a sliding discharge. The PM oxidation efficiency was improved by increasing the applied AC high voltage of the surface discharge and the ambient temperature. These results suggest that the novel aftertreatment system can be in practical use with further improvement of PM oxidation efficiency.

## Acknowledgement

The authors are grateful to TOYOTA MOTOR Corp. and TOYOTA INDUSTRIES Corp. for the support given to this work. The authors also thank to the supply of the electrodes to KYOCERA Corp.

## 5 Literature

- [1] D. B. Kittelson; Engines and Nanoparticles: A Review ; Journal of Aerosol Society; Vol. 29; No. 5/6; pp. 575-588; 1998
- [2] A. Zukeran, Y. Yasushi, Y. Ehara, T. Ito, T. Takahashi, H. Kawakami, and T. Takamatsu; Agglomeration of Particles by ac Corona Discharge; Electrical Engineering in Japan; Vol. 130; No. 1; pp. 30-37; 2000
- [3] K. Hanamura and T. Tanaka; Visualization study of heterogeneous reaction of particulate matter in regeneration of DPF; Proceedings; JSAE Annual Congress; No. 22-05; pp. 23-26; 2005
- [4] M. Okubo, S. Miwa, T. Kuroki and T. Yamamoto; Low Temperature Soot Incineration of Diesel Particulate Filter Using Honeycomb Nonthermal Plasma; Transactions of the Japan Society of Mechanical Engineers; Part B; Vol. 69; Issue 688; pp. 2719-2724; Dec. 2003 (in Japanese)
- [5] K. Hensel, S. Sato and A. Mizuno; Sliding Discharge Inside Glass Capillaries; IEEE Transactions on Plasma Science; Vol.36; No.4; pp. 1282-1283; Aug. 2008
- [6] S. Sato, K. Hensel, H. Hayashi, K. Takashima and A. Mizuno; Honeycomb discharge for diesel exhaust cleaning; Journal of Electrostatics; Vol. 67; pp. 77-83; 2009
- [7] C. Louste, G. Artana, E. Moreau and G. Touchard; Sliding discharge in air at atmospheric pressure: electrical properties; Journal of Electrostatics; Vol. 63; pp. 615-620; 2005
- [8] S. Sato and A. Mizuno; NO<sub>x</sub> Removal of Simulated Diesel Exhaust with Honeycomb Discharge; International Journal of Plasma Environmental Science

and Technology; Vol.4; pp. 18-23; Mar.  
2010